Growth rates of oceanic manganese nodules: Implications to their genesis, palaeo-earth environment and resource potential

B. L. K. Somayajulu
Physical Research Laboratory, Ahmedabad 380 009, India

Cosmic ray produced ^{10}Be has provided the most reliable method of determining growth rates of oceanic ferromanganese nodules/encrustations of age < ~ 15 m.y. The uses of this parameter to understand the genesis and resource potential of these deposits and for using them as recorders of palaeo-events are briefly described.

Discovered more than 125 years ago during the Challenger Expedition[1], oceanic manganese nodules also known as ferromanganese nodules/deposits and polymetallic nodules (this mineral group also occurs in the form of encrustations) continue to fascinate scientists from various disciplines. Explanations concerning their origin and occurrence mainly on the top (~ 50 cm) of the oceanic sedimentary column, and technologies required to be developed for economically mining these potentially resourceful minerals from the abyss are some of the problems that deserve fresh look. This does not mean that manganese nodules were elusive to researches which have been carried out intensely between the fifties and late eighties. These yielded a huge amount of data[2–5] concerning their composition, mineralogy, growth rates and usefulness as indicators of palaeo-events[6–8] that took place in the ocean, on the earth and in interplanetary space[9,10]. These data form a solid base for further studies of these deposits to gain a deeper understanding.

In this review, a brief account of the basic information on manganese nodules is presented with emphasis on their growth rate determination mainly using cosmic ray produced ^{10}Be (half life = 1.5 m.y.). Growth rate of nodules are very useful in providing clues to the origin and occurrence of these deposits, their usefulness as recorder of past-sea water chemistry/oceanography, the earth's magnetic field and cosmic ray intensity variations and in assessing their resource potential.

Occurrence

In the nodular/concretion form which is by far the most common mode of occurrence, this deposit occurs in irregular spheroidal/ellipsoidal shape, with diameters (or the longest side) measuring ~ 1 to 5 cm[2–6,11] (Figure 1). If a nodule is sliced into two halves, the radial cross-section (Figure 2) clearly indicates that the growth of oxy-hydroxides of Mn and Fe takes place on an object, viz. some kind of core material like ear bone, sharks tooth or a piece of basalt, palagonite, etc. Larger ferromanganese nodules (dia > 5 cm) exist, but they are rare. It should also be pointed out that most of the nodules irrespective of their size occur at the top ~ 50 cm of the sediment pile[11–13].

In the form of encrustation (Figure 3 *a* and *b*), the deposit grows on hill slopes and rocky surfaces where the size can be very large. Most of the nodules/encrustations are collected by dredging using chain dredges[2–5]. In module-dominated areas, box cores were collected with nodules present at the top in growth positions[14]. Recent studies in the Pacific have shown that the growth of ferromanganese encrustations in terms of their composition is independent of the basal rock[15].

The basal material on which the encrustations grow is generally (altered) basalt (Figure 3 *b*).

Mineralogy and composition

The two principle elements of the ferromanganese deposits as the name reveals, are Mn and Fe which occur in the following mineral forms[16,17]:

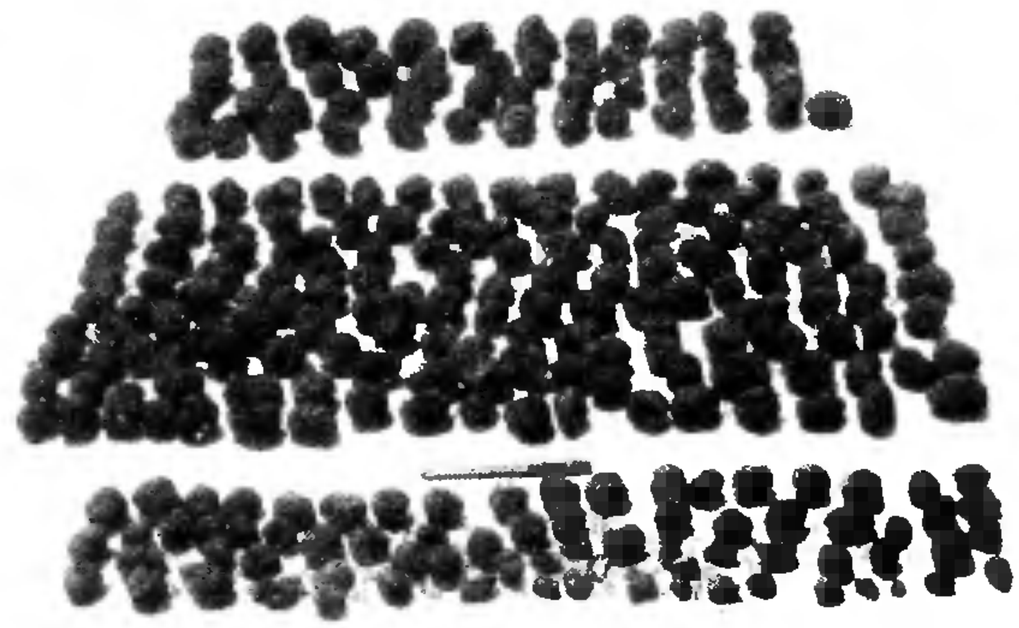

Sample No. 280 U
SS4

Figure 1. Manganese nodules/concretions collected from the Central Indian Ocean Basin. These are the most commonly occurring sizes.

e-mail: soma@prl.ernet.in

Mn: δMnO_2, Birnessite (Ca, Na) (Mn^{2+}, Mn^{4+}), $O_{14}{\cdot}3H_2O$, Todorokite (Na, Ca, K, Ba, Mn^{2+})$_2{\cdot}Mn_5O_{12}{\cdot}3H_2O$
Fe: Goethite α Fe O (OH)

Most of the minerals of minor elements also occur (see refs 4, 5, 16, 17 for details). It is to be noted that δMnO_2 occurs more commonly than birnessite and todorokite.

Compositionally Mn and Fe are the major elements with Cu, Co, Ni, Zn and a host of others ranging from minor to trace levels. One common feature of ferromanganese deposits is their compositional heterogeneity[4,5,18]. Nodules from the three oceans differ and there are large differences even from the same general region of any ocean. Composition depends also on the mineralogy which is depth dependent[19]. These differences, as will be briefly discussed later, are due to the sources of the elements, the post depositional reactions, e.g. diagenesis, etc.[20]. To get an idea about the composition of the ferromanganese deposits, world average values are listed in Table 1.

Mode of formation

Right from the time nodules were discovered[1], there have been theories concerning their origin. As a starting point, the (catalytic) oxidation process put forward by Goldberg[21] and others[20,22] can be considered.

$$Mn^{2+} + 2\,OH^- + \tfrac{1}{2}\,O_2 \rightarrow MnO_2 + H_2O$$
$$Fe^{3+} + OH^- + \tfrac{1}{2}\,O_2 \rightarrow FeO\,(OH),$$

Once the oxyhydroxides of Mn and Fe start forming on a suitable object at the sediment–water interface, incorporation of other metals by scavenging and other processes involving bacterial mediation could be worked out. The problem then boils down to finding ways and means of making Mn and Fe available at the site of nodule formation. The sources could be (i) dissolved Mn and Fe in sea water which are entering the ocean as weathering solution provided by rivers and streams, (ii) sedimentary Mn and Fe that diffuse out of pore waters through diagentic processes, and (iii) hydrothermal/submarine volcanic contributions of Mn and Fe[23]. Mn and Fe from sources (ii) and (iii) could yield faster growth rates of manganese deposits. One of the much-needed parameters for a reasonable understanding of the origin and modes of occurrence of manganese nodules is their growth rate(s).

Growth rates

The articles by Ku (in refs 4 and 5) give a comprehensive account of methods applied for determining nodule/encrustation growth rates; more data especially using ^{10}Be and other chemical methods have been obtained during the past decade and half.

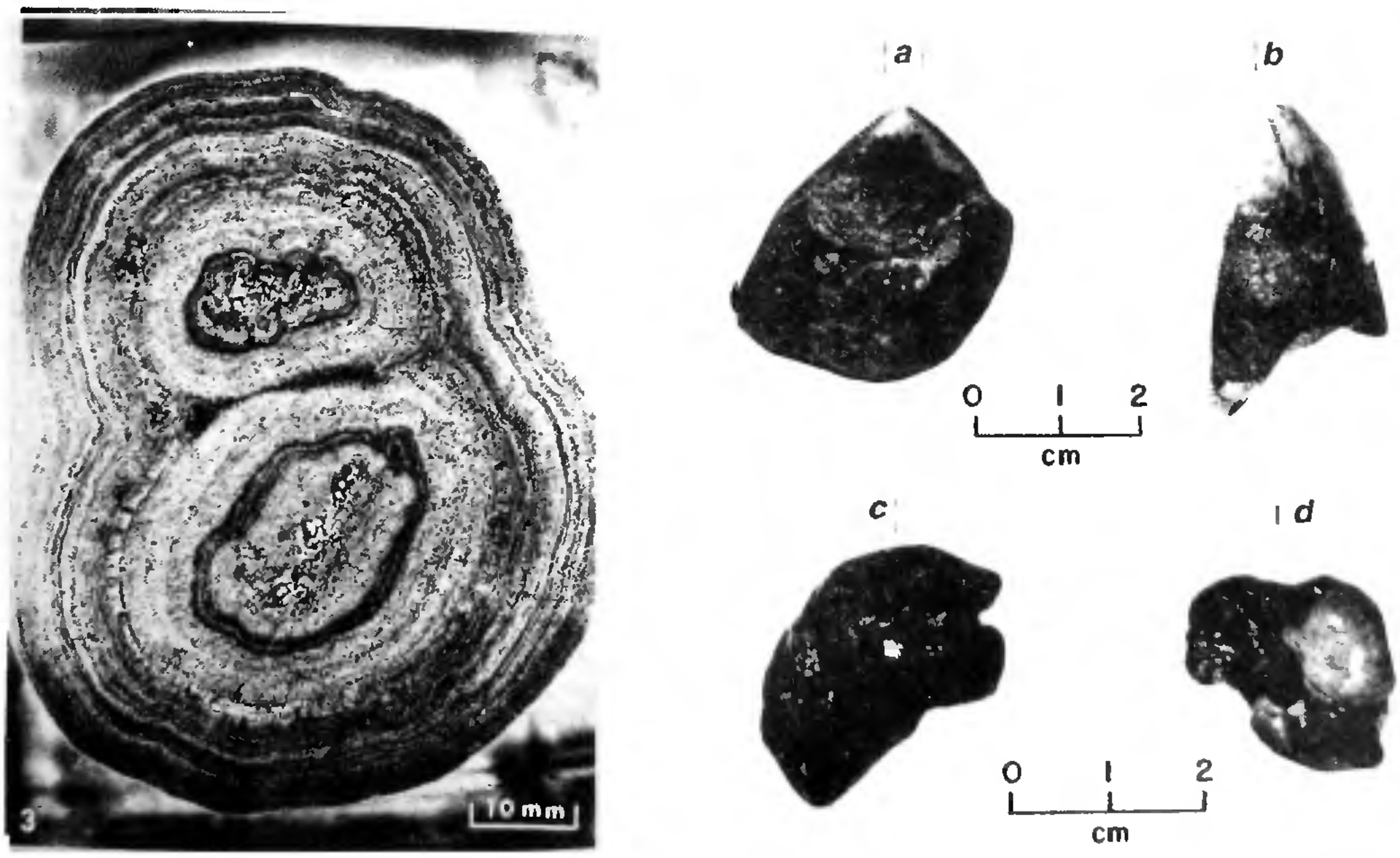

Figure 2. (*Left*) Polished cross-sections of a Pacific ocean nodule indicating that two nodules coalesced as they were growing[68]. The two cores and the Mn and Fe oxyhydroxide layers deposited on them are clearly seen. (*Right*) ***a***, Sharks's tooth; and ***b***, cetacean ear bones[3]. These also form the cores of nodules.

Basically, there are two ways of determining the nodule/encrustation growth rates: (i) applying various methods to the crust, and (ii) date the cores with the explicit assumption that crustal growth started ever since the core material, e.g. shark's tooth or basalt piece, etc. came into existence as an independent entity on the top of the oceanic sediment column. It is also seen that there are fewer methods for dating nodule cores. Growth rates derived using method (ii) will in general be on the lower side. An account of all methods applied for growth rate determination of the ferromanganese deposits are listed in Table 2.

All methods (Table 2) yielded growth rates in the range of < 1 mm to ~ 100 mm/m.y. Growth rates based on the analysis of crustal material are the most appropriate ones. The most commonly employed radioisotope for determining growth rates of nodules was ^{230}Th (Ku's articles in refs 4 and 5), the main limitation of this method is the short half life of ^{230}Th (Table 2). It can be applied to the top < 1 mm of the manganese crust whereas the nodules in general, are at least a few cm (if not larger) in diameter. The most suitable method is based on ^{10}Be which can be measured throughout several cm thick crusts, a brief account of which is given in the next section.

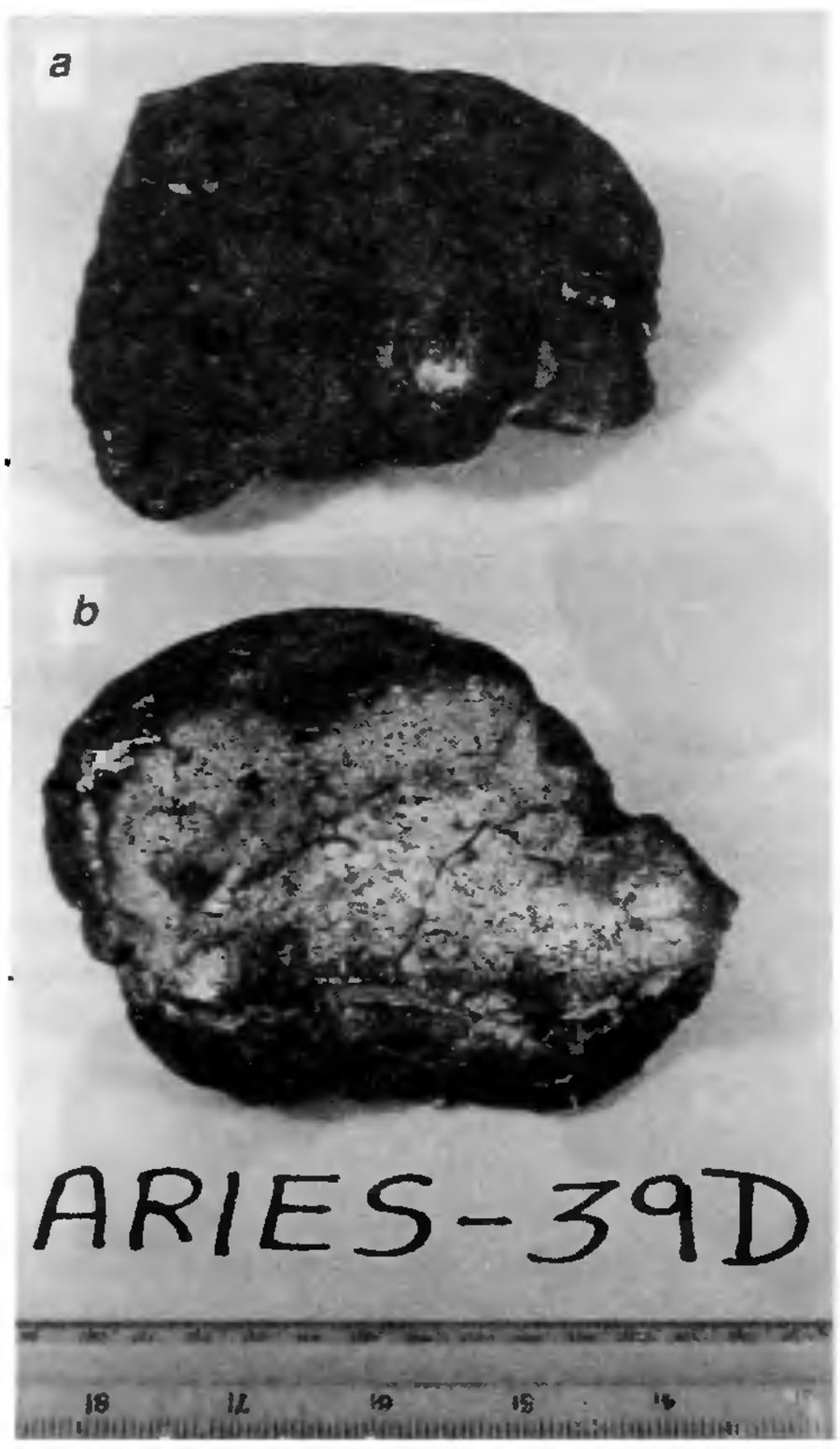

Figure 3. Encrustation from the Pacific: *a*, top side; and *b*, bottom side.

^{10}Be method

Cosmic ray produced ^{10}Be (Table 1) in the atmosphere by interaction of protons and neutrons (secondaries) with nitrogen and oxygen[24] reaches the earth predominantly through rain and snow. The ocean gets ^{10}Be either by direct rainfall, molten ice inputs and some by river and stream run-off. Being a reactive element, Be (^{10}Be) gets removed from water by adsorption on detrital material, mainly clay and reaches the underlying sediments in times very short (~ 300 years)[25] compared to its half life. Long-lived radioisotopes of reactive elements (in the ocean) like ^{230}Th and ^{10}Be are enriched in deep sea sediments which led to the development of dating methods for marine sediments using ^{10}Be (ref. 26) and ^{230}Th (ref. 27). From the available and very limited data on stable Be concentration in sea water[28] and in one manganese nodule Somayajulu[29] calculated that in terms of ^{10}Be, every gram of ferromanganese crust is equivalent to ~ 10 metric tons of sea water, reasoned that one should be able to measure this radionuclide (based on its estimated steady state inventory in sea water[24]) in ~ 100 g manganese crust and detected it in a Pacific manganese encrustation. Since then the ^{10}Be method of dating manganese nodules was pursued by only four groups[30–33], mainly due to a large sample requirement. After the inception of the AMS

Table 1. Average concentration, inventory and annual deposition of some important elements in ferromanganese nodules

Element	Average concentration in nodules*	Inventory in nodules† (g)	Deposition rate** (g/yr)
Mn	18.6%	2.6×10^{17}	2.6×10^{10}
Fe	13.6%	1.9×10^{17}	1.9×10^{10}
Ni	0.55%	7.7×10^{16}	7.7×10^{9}
Cu	0.34%	4.8×10^{15}	4.8×10^{8}
Co	0.27%	3.8×10^{15}	3.8×10^{8}
Zn	0.12%	1.7×10^{15}	1.7×10^{9}
La	108 ppm	1.5×10^{14}	1.5×10^{7}
Ce	510 ppm	7.2×10^{14}	7.2×10^{7}
Nd	152 ppm	2.1×10^{14}	2.1×10^{7}
Sm	36 ppm	5.1×10^{13}	5.1×10^{6}
Eu	8.4 ppm	1.2×10^{13}	1.2×10^{6}
Gd	35 ppm	4.9×10^{13}	4.9×10^{6}
Dy	31.5 ppm	4.4×10^{13}	4.4×10^{6}
Er	16.8 ppm	2.4×10^{13}	2.4×10^{6}
Yb	15.3 ppm	2.2×10^{13}	2.2×10^{6}
Th	25 ppm	3.5×10^{13}	3.5×10^{6}
U	10 ppm	1.4×10^{13}	1.4×10^{6}
Os	1.4 ppm	2.0×10^{12}	2.0×10^{5}
Ir	10 ppb	1.4×10^{10}	1.4×10^{3}
Au	3 ppb	4.2×10^{9}	4.2×10^{2}
PD	6 ppb	8.4×10^{9}	8.4×10^{2}

*World ocean average data collected from refs 18–20, 70–74.
†Estimated using the area of the ocean floor occupied by the nodules as 10% of the total, viz. 3.6×10^{17} cm^2, thickness of the nodule deposit is 2 cm and density is 1.95 g/cm^3 (ref. 11).
**Using a mean growth rate of 2 mm/10^6 yr (Figure 5).

technique[34,35] and later the SIMS[36] (Table 2) to make ^{10}Be measurements, the sensitivity of this method has tremendously improved by almost six orders of magnitude. With < 50 mg sample and simple radiochemistry, one can measure ^{10}Be effortlessly in nodules and sediments. Since then the ^{10}Be method has been extensively used by many groups.

The procedural details for deducing the growth rate of manganese nodule/encrustation consist of measuring ^{10}Be concentration as a function of depth and making log-linear plot of radionuclide activity versus depth (Figure 4). Usually such plots are straight lines, the slope (λ/S where λ the ^{10}Be decay constant = 4.62×10^{-7} year^{-1} and S is the growth rate in mm/y) yields the growth rate. The exponential decrease of radioactivity with depth is interpreted in terms of the following models[32,37].

Growth model

This assumes that the nodule remains in a closed system since it starts growing around an object (core material, Figure 2) and that the decrease in the radio-isotope concentration is due to its decay. The mathematical formulation is

$$S\frac{dC}{dZ} - \lambda C = 0. \quad (1)$$

The solution is

$$C = C_0 \exp\left[-\left(\frac{\lambda}{S}\right)Z\right], \quad (2)$$

Table 2. Methods for growth rate determination of oceanic ferromanganese deposits

Method	Dating interval (year)	Principle	Measurement technique(s)	Refs
Crust-based methods				
^{230}Th	10^3–10^5	Decay of unsupported $^{230}Th_{xs}$ (half life = 7.52×10^4 year) of $^{230}Th_{xs}/^{232}$Th; $^{230}Th_{xs}$ normalized to ^{232}Th (= 1.4×10^{10} year) with depth < ~ 1 mm	Radiochemistry followed by alpha spectroscopy or thermal ionization mass spectrometry. Recording α tracks on cellulose nitrate sheets, and developing and counting them using optical microscope	47, 75, 76
^{231}Pa, ^{230}Th/^{231}Pa	10^3–10^5	Decay of unsupported $^{231}Pa_{xs}$ (=3.25×10^4 year) or unsupported activity ratio of $^{230}Th_{xs}/^{231}Pa_{xs}$ (= 5.71×10^4 year) with depth < ~ 1 mm	Radiochemistry followed by alpha spectroscopy	47, 77
^{10}Be	10^5–10^7	Decay of cosmic ray produced ^{10}Be (= 1.5×10^6 year) with depth ≤ 100 mm	Radiochemistry followed by beta assay or radiochemistry followed by accelerator mass spectrometry or secondary ion mass spectrometry	29, 34, 36, 36a
^{26}Al, ^{26}Al/^{10}Be	10^4–10^6	Decay of cosmic ray produced ^{26}Al (= 7.16×10^5 year) and/or ^{26}Al/^{10}Be (= 1.37×10^6 year) with depth < ~ 50 mm	Radiochemistry followed by AMS	30, 78
Mn/Fe	10^5–10^7	Mn/(Fe)^2 concentration is linearly correlated with growth rate of nodule crust.	Measurement of Mn and Fe concentrations by standard techniques	79
Co	10^5–10^8	In hydrogenous manganese crusts growth rate is inversely correlated to Co concentration	Measurement of Co using standard techniques	40, 80
^{87}Sr/^{86}Sr	10^6–10^8	Comparing ^{87}Sr/^{86}Sr ratio of Mn crustal layers with its evolution in sea water with time	Measuring ^{87}Sr/^{86}Sr in the hydrogenous Mn crusts as a function of depth using TIMS	81
Magnetic reversal	10^5–10^7	Chronology of the reversal in earth's magnetic field direction established. Sequential detection of normals and reversals of NRM direction will yield ages for the respective depths of detection	Measurement of the intensity and direction of the natural remanent magnetism with respect to chosen (vertical) direction using Astatic and/or spinner magnetometers	62, 82
Core-based methods				
K–Ar	10^5–10^9	Decay of naturally occurring ^{40}K (which is 0.012% of K) by electron capture and positron emission into ^{40}Ar with a half life of 1.26×10^9 year in the basaltic material. K and ^{40}Ar measurements yield the age	Mass spectrometry for ^{40}Ar and atomic absorption spectrophotometry for K	83
Amino acid racemization	10^3–10^6	Rate of racemization of amino acid L-isoleucine to D-alloisoleucine is slow and well determined so that ratio of alleu/iso can yield age (half life of reaction is 290,000 year, i.e. alleu/iso = 0.345)	Chemistry followed by measurement of L and D varieties by amino acid analyser in successive layers of carefully sampled crust	84, 85

XS, Excess; $^{230}Th_{xs} = {}^{230}Th_{Total} - {}^{234}U$ (all in units of dpm/g); $^{231}Pa_{xs} = {}^{231}Pa_{Total} - {}^{235}U$ (all in units of dpm/g).

where C and C_0 are concentrations of the radioisotope in question (^{10}Be in the present discussion) at depth Z (mm) and at the very surface, respectively. Changes in slope of the line (Figure 4) indicate changes in growth rates.

Diffusion model

Another way of looking at the log-linear plot is by the consideration that the radioisotope in question is actually diffusing into a pre-existing (obvious assumption) nodule/encrustation from the surface to the inside. The equation for such a diffusion model is

$$K\frac{d^2C}{dZ^2}-\lambda C=0, \tag{3}$$

for which the solution is

$$C=C_0\exp\left[-\left(\frac{\lambda}{K}\right)^{1/2}Z\right], \tag{4}$$

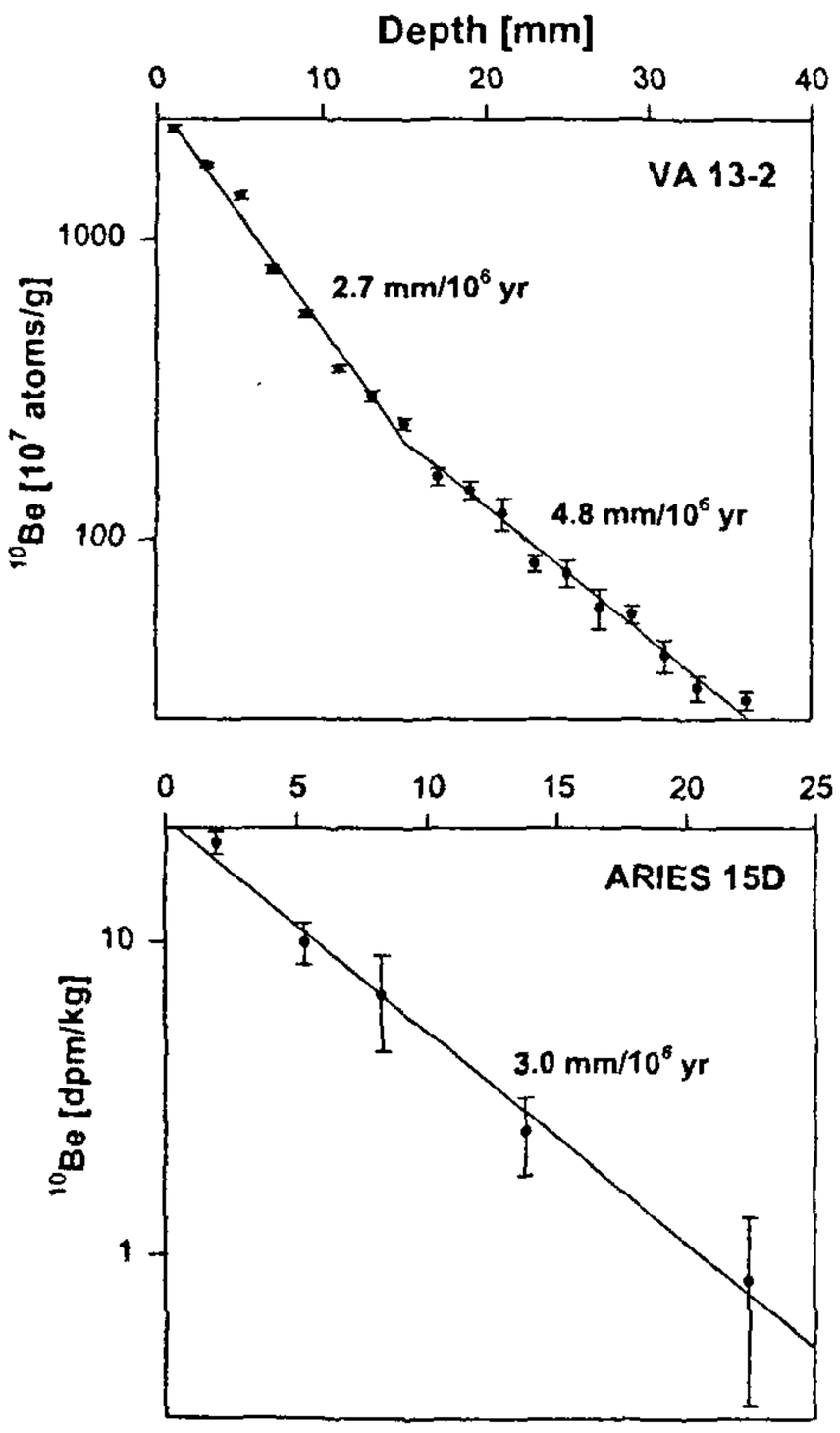

Figure 4. Log-normal plots of ^{10}Be vs depth in encrustations from the Pacific. Top and bottom plot denote ^{10}Be measurements using AMS[6] and radiochemistry followed by beta assay[42], respectively. Change in slope (top figure) indicates change in growth rate.

where K is the diffusion coefficient (cm^2/s). The fact that growth rates determined by radionuclides of widely differing half lives[32] and physical and chemical properties (by other physical and chemical methods too (Table 2)) are in good agreement and the calculated K values $< 1\times 10^{-8}$ cm^2/y (ref. 38) rules out the diffusion model as the plausible mechanism.

Growth and diffusion model

This takes both growth and diffusion models into account.

$$K\frac{d^2C}{dZ^2}-S\frac{dC}{dZ}-\lambda C=0, \tag{5}$$

which has the solution

$$C=C_0\exp\left[\frac{S-(S^2+4K\lambda)^{1/2}Z}{2K}\right]. \tag{6}$$

Ku *et al.*[39], who first applied this model observed that the growth rate obtained using ^{10}Be, ^{230}Th and ^{231}Pa (Table 2) in a module followed the pattern, ^{10}Be < ^{230}Th < ^{231}Pa which shows that lowest growth rate is obtained using ^{10}Be and that processes such as diffusion and mixing are more due to sampling of very thin layers and very irregular nodule encrustation surfaces and that radioisotopes with shorter half life will be more affected by these[32]. Overall, ^{10}Be-based growth rates are about the most reasonable with no appreciable contribution from diffusional effects[38].

While extending the ^{10}Be-based growth rates to deeper depths (in nodules) older than ~ 12 m.y., it has been observed that Co-based rates[40] (Table 2) show promise and are being used in some cases[41]. It seems appropriate to add here that all the earlier ^{10}Be-based growth rates using radiochemistry and beta assay[31,35,42] are confirmed by AMS[6,43,44] and later by SIMS[45] ^{10}Be measurements and the dating range extended to ~ 15 m.y. (ref. 46). A fairly up-to-date data on the distribution of ^{10}Be-based growth rates of manganese nodules/encrustations from world oceans are shown in Figure 5. Ku and Broecker[47], based on growth rate determination using U–Th decay series' nuclides postulated that the growth rates of authigenic/hydrogenous ferromanganese deposits are by far the slowest < 6 mm/m.y. Almost all ^{10}Be-based growth rates (Figure 5) measured on the hydrogenous variety fall within this range. Beyond the ^{10}Be range, for larger nodules/thick encrustations, the Co method has been found to yield satisfactory growth rates on select samples[41].

Since growth rates of ferromanganese deposits are determined, the implications of such rates to various aspects of nodule formation and environment are being studied at several laboratories in the world. An account of these studies is now briefly described.

Genesis of ferromanganese deposits

In the earlier section, three sources of Mn and Fe for nodule formation were mentioned. In the case of the Apple nodule, it has been shown that the growth rate of the surface facing pore waters is faster than the other facing sea water[48]. Diagenesis that should be more prevalent on the sediment-facing side, can help in accelerating nodule growth rates. In two separate studies using $^{230}Th_{xs}$ and $^{231}Pa_{xs}$, on different-oriented manganese nodules, it was found that in one, there was no difference in growth rates of top and bottom (sediment facing) sides[14], whereas in the other[48] the bottom side was growing faster by over a factor of two. However in both studies, the concentration of $^{230}Th_{xs}$ and $^{231}Pa_{xs}$ was higher by several factors in the top sides compared to the bottom side. By analogy, ^{10}Be is expected to be enriched in the top side of oriented nodules. Nodules/encrustations from hydrothermal/volcanic sites have by far the fastest (orders of magnitude) growth rates due to abundant supply of Mn and Fe[49]. As suggested by Ku and Broecker[47] and by all ^{10}Be measurements (Figure 5) slow growth rates, < 10 mm/m.y., most likely indicate authigenic/hydrogenous mode of formation for these deposits.

Another observation concerning the occurrence of manganese nodules (not encrustation unless they are broken and the pieces are lying on the top of the sediment pile) only is their maximal abundance in the near-surface regions with almost negligible amounts at depths > 50 cm. Since marine sediments accumulate 2–3 orders of magnitude faster than the nodules, the latter should have been buried, i.e. present in deeper levels. Earlier workers[13,31,42,47] too have addressed this problem and suggested mechanisms, which are summarized below:

(i) In many nodule field (sediment tops) photographs one notices ripple marks on sediments[2] indicating the presence of currents that can move sediments without disturbing the nodules appreciably. These currents can also erode nodule surfaces which was noted in the south-east Indian ocean[50]. Time-lapse photographic observations[51] revealed the presence and movement of crabs, holothurians and other organisms which could cause bioturbation that would result in keeping nodules afloat on the sediment column and can also account for spheroidal/concretionary shapes of the deposits.

If the nodules are growing (as revealed by the techniques listed in Table 2) and are eroding, the net growth would have to be small. The net growth could be < 25% of the possible total growth as evidenced by depleted (by about a similar factor) $^{230}Th_{xs}$ and ^{10}Be inventories in the nodules compared to the expected values from the overhead sea water column. Of the expected 1 dpm $^{10}Be/cm^2$ from cosmic ray production[33] and 1000 dpm $^{230}Th/cm^2$ from the ^{238}U inventory of sea water[47], the measured inventories are < 25% of the expected ones. It should be noted here that marine sediments generally do not show this discrepancy, the expected and measured inventories of ^{10}Be and ^{230}Th are in good agreement.

(ii) Another equally plausible explanation is that nodule growth is limited to a few 100 m bottom water column[42] and certainly not the entire water column like in the case of marine sediments. In areas of high biological productivity like the Arabian Sea, due to the anoxicity created in the subsurface and in deep waters (for example denitrification in the north-eastern Arabian Sea[51,52]), Mn and Fe (to a smaller extent) would be in the lower oxidation state which is not favourable to ferromanganese deposit formation. It is equally possible that all the above-mentioned mechanisms are operative, their relative importance, however, would be site-specific.

Palaeo-studies using manganese nodules/encrustations

Since nodules, especially smaller ones (< 5 cm dia), have the problem of turnover/rotation on the seafloor, they may

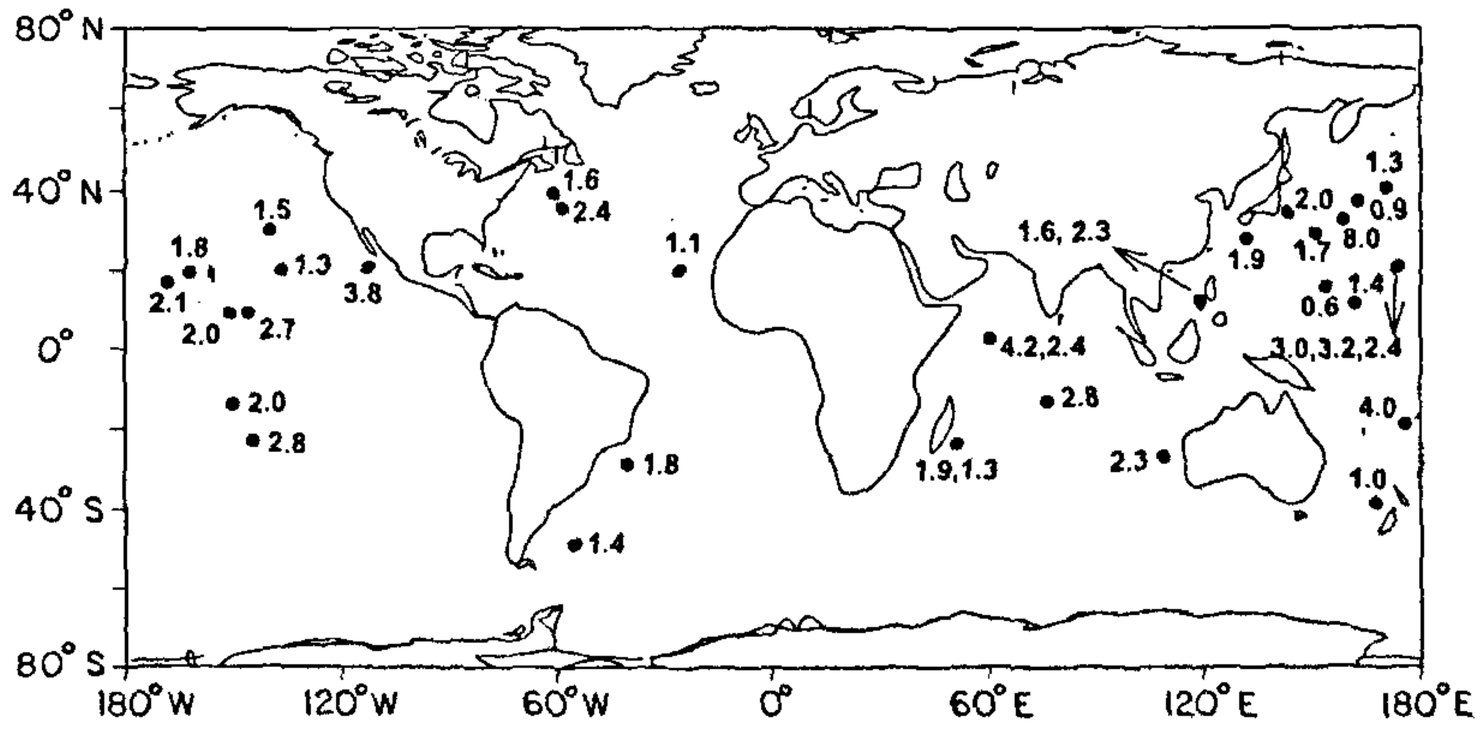

Figure 5. ^{10}Be based-growth rates of ferromanganese deposits (in units of mm/10^6 yr) from world oceans using all the three measurement techniques, viz. beta-assay, AMS and SIMS (Table 1). Data are collected from refs 6, 8, 30, 32, 33, 35, 37, 38, 41–46, 69.

not be sampling sea water column during their entire period of existence. If flipped, they would be in closer contact with pore waters and the growth rate as well as the flux of metals into them would then increase[48]. Because they are free from this problem, most of the palaeo-studies have been confined to sea mount encrustations. Dated ferromanganese encrustations sampled continuously at narrow (~ 1 mm) intervals will reveal the palaeo-information (sea water chemistry, changes in ocean circulation) through variations exhibited by diagnostic elemental and isotopic measurements. For example, using structural and transition metal composition of dated layers of a Mn crust from the central North Pacific, Segl *et al.*[6] were able to show that crustal growth was influenced by palaeo-climate which had implications to palaeo-circulation. In a dated manganese encrustation (using extrapolated ^{10}Be growth rates) from north-western Pacific, it was found that highly positive Ce anomalies[53] and high Ir concentration[54] were found at depths older than 50 m.y., indicating that the bottom waters of the region were relatively more oxic and that the nodule would have started growing from around K/T times.

The Oxford group along with others has dated several manganese encrustations[8,45,46,55] from the Pacific, Atlantic and Indian Ocean using ^{10}Be and extended it beyond using the Co method in some suitable cases. The highlights of these studies are:

(i) Ascertaining the past aeolian and fluvial inputs of terrestrial material into the ocean, e.g. to the Labrador Sea in the North Atlantic; (ii) Changes in ocean circulation due to opening and closing of gateways, e.g. restriction of the Panamanian gateway from 10 m.y.BP with final closure at 3–5 m.y.BP decreased the North Atlantic Deep Water (NADW) component to the Pacific; (iii) Increase in NADW production before 7 m.y.BP; (iv) Record of Himalayan erosion during the last ~ 20 m.y. which would effect the chemistry of the Indian Ocean water and ultimately the world ocean water in case elements with long residence times like Sr (in the form of ^{87}Sr/^{86}Sr (ref. 56)).

Changes in the earth's past magnetic field and cosmic ray intensities

This has been a topic of interest during the past three decades[57-59] and the recorders for these variations have been deep sea sediments. Well-dated deep sea sediments in principle record ^{10}Be changes which could be due to several causes including climatic[57,59–61]. It is now possible to use sea mount manganese encrustations to study these intensity variations. In principle, what one looks at is the variation of decay corrected ^{10}Be or ^{10}Be/^{9}Be in successive layers of well-dated nodules. The NRM intensities can also be measured so that one can correct the decay corrected ^{10}Be data for magnetic field intensity[62] variations and attribute the remainder to CR intensity variations[60]. The decay corrected parameter ^{10}Be/^{9}Be is plotted as a function of time, viz. age of each layer (relative to surface) for the past ~ 12 m.y. (Figure 6). It should be pointed out here that the age is determined by ^{10}Be decay only. The best fit lines to the ^{10}Be data yield the average growth rate for each encrustation (see references given in Figure 6). Using growth rate, the age is obtained for each sample with which the ^{10}Be data are decay corrected. It is seen that the decay corrected ^{10}Be/^{9}Be increased by a factor of ~ 1.5 during the past ~ 1.5 to ~ 4 m.y.BP. This happened in three of the six encrustations selected. These changes can be attributed to a combination of magnetic field[60,63,63a] and CR intensity variations. The increase in CR intensity could be due to a nearby supernova explosion[56] and/or decrease in the earth's magnetic field intensity. The present analysis only indicates that there is a possibility to look for these changes up to the past ~ 15 m.y. which in terms of encrustation would be ~ 5 cm. One notes in Figure 6 that the ^{10}Be/^{9}Be ratio in the surface section of the encrustations (which represent past ~ 1 m.y.) varies by a factor of over 5. These variations are due to various oceanic processes, ^{10}Be sources, etc[59]. In the present discussion, we are considering only the ^{10}Be/^{9}Be variation with depth (i.e. time) at each location. In view of the observation that post-depositional processes, viz. diagenesis[64] could affect records at micron levels and due to unevenness of the nodule/encrustation surfaces[32] it is not possible to sample nodule/encrustation layers thinner than ~ 1 mm. The studies carried out so far show that a wealth of palaeo-information can still be derived from ferromanganese deposits.

One has to look for the oldest nodules/encrustations that could take the records back to at least ~ 100 m.y. to understand evolution of ocean chemistry and circulation and continental weathering through time.

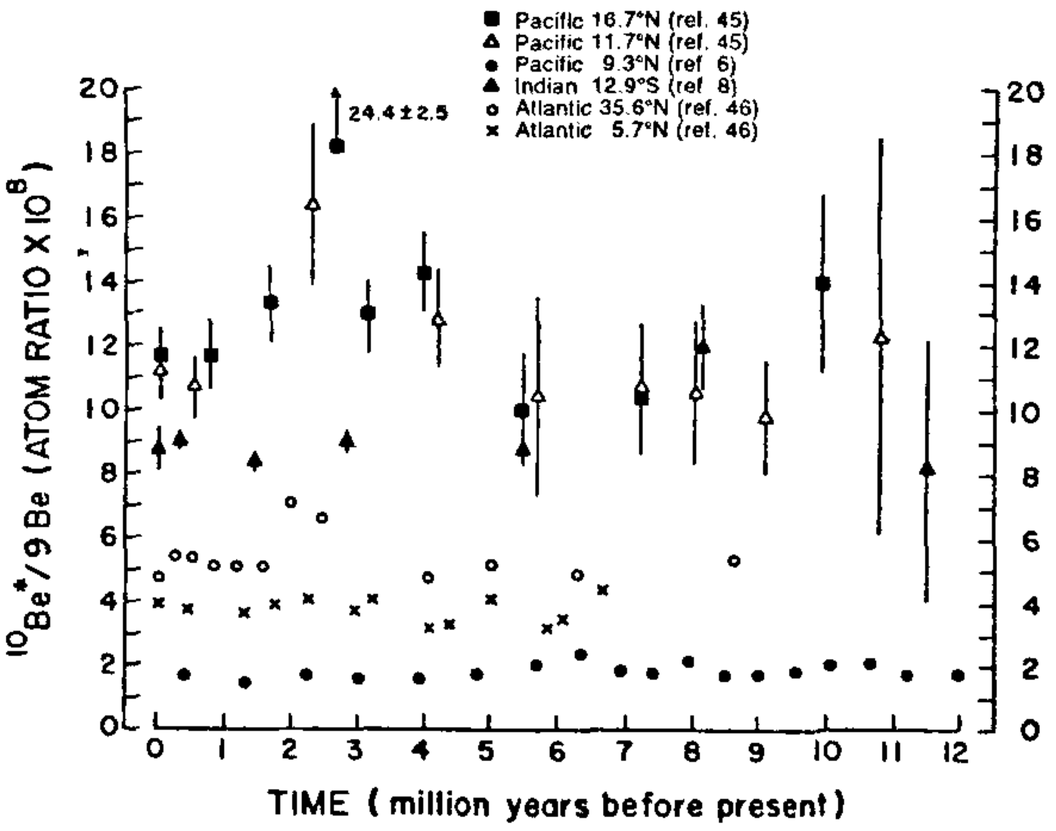

Figure 6. Decay corrected ^{10}Be/^{9}Be ratio as a function of time in the past for six ferromanganese encrustations from the Pacific. In three of the six encrustations there is a peak ~ 2 to ~ 4 m.y.BP.

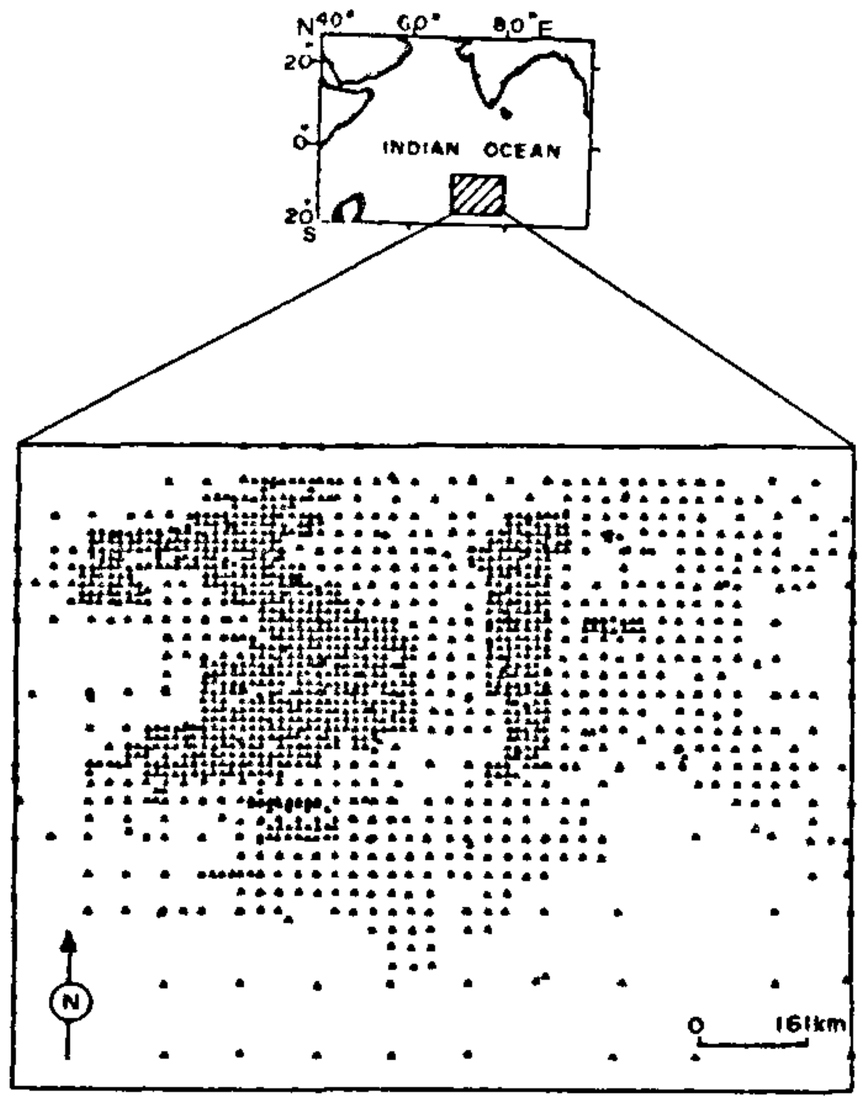

Figure 7. Two sites identified for mining the Central Indian Ocean Basin[66].

Resource potential

There are several books available on ferromanganese deposits as a resource and their economic potential[2–4,17,65]. Here only growth rate-based evaluation of resource potential is discussed. From the world oceanic area covered with manganese mineral, its thickness and mean composition, one can estimate the inventory of elements in these deposits. This is done (Table 1) taking the average thickness of the deposit (whether in the form of nodule/concretion or encrustation) to be 2 cm. This, most likely, represents a lower limit. Knowing the growth rate, the annual deposition of various elements in the form of ferromanganese deposits is also calculated (Table 1). One notes that a significant amount of metals are deposited annually in the form of ferromanganese deposits. One question that comes up is as follows: If manganese nodules are mined, will they start growing again? As long as the core material (Figure 2) on which nodules grow exists at deep layers of sediments too (assuming the top ~ < 5 m of sediment is lost/displaced during nodule mining), there is no reason why nodule formation should cease. In India, the Department of Ocean Development, mostly through studies carried out at the National Institute of Oceanography, Goa made much progress in this connection having identified two potentially minable sites, in the Central Indian Basin (CIB, Figure 7)[66]. Once a reasonable mean concentration and growth rate[35] are deduced, the inventory as well as the annual accumulation of economically important metals in CIB can be estimated.

In summary, growth rate determination of oceanic ferromanganese deposits has helped in delineating their modes of formation and in ascertaining the annual growth of this potential resource. One can also use them as recorders of palaeo-events – oceanic (chemistry, circulation, etc.), terrestrial (weathering) and extra-terrestrial (magnetic field and intensity) and their variations during the past < 15 m.y. Collection of thicker (10–20 cm) ferromanganese encrustations, dating with ^{10}Be and Co and looking for Ir, Os, Sr and Nd isotopic signatures[61,67] to gain better understanding of events like cretaceous–tertiary (K/T) transition and its manifestations, temporal changes in weathering regimes, ocean chemistry, circulation, etc. could be our future endeavours in this field.

1. Murray, J. and Renard, A. F., in Report of the Scientific Results of the Exploration Voyage of the H.M.S. Challenger Expedition (eds Thompson, C. W. and Murray, J.), London, 1891, p. 583.
2. Mero, J. L., *The Mineral Resources of the Sea*, Elsevier, Amsterdam, 1965.
3. Horn, D. R. (ed.), *Ferromanganese Deposits on the Ocean Floor*, LDGO, NY, IDOE/NSF, Washington D.C., 1972.
4. Glassby, G. P. (ed.), *Marine Manganese Deposits*, Elsevier, The Netherlands, 1977.
5. Bischoff, J. L. and Piper, D. Z. (eds), *Marine Geology and Oceanography of the Pacific Manganese Nodule Province*, Plenum Press, New York, 1979.
6. Segl, M., Mangini, A., Bonani, G., Hofman, H. G., Nessi, M., Suter, M., Wolfli, W., Friedrich, G., Pluger, W. L., Wiechowski, A. and Beers, J., *Nature*, 1984, **309**, 540–543.
7. Sharma, P. and Somayajulu, B. L. K., in *Contributions in Marine Sciences – Dr S. Z. Qasim's 60th Birthday Memorial Volume* (eds Rao, T. S. S., Natarajan, R., Desai, B. N., Swami, G. N. and Bhat, S. R.), Ujjvala Printers, Bombay, 1987, pp. 355–380.
8. Frank, M. and O'Nions, R. K., *Earth Planet. Sci. Lett.*, 1998, **158**, 121–130..
9. Finkelman, R. B., *Science*, 1970, **167**, 982–984.
10. Jedwab, J., *Meteoritics*, 1975, **10**, 191–207.
11. Greenslate, J. L., *Mar. Min.*, 1977, **1**, 125–148.
12. Menard, H. W. and Shipek, C. J., *Nature*, 1958, **182**, 1156–1157.
13. Heath, G. R., *Science*, 1979, **205**, 903–904.
14. Krishnaswami, S. and Cochran, J. K., *Earth Planet. Sci. Lett.*, 1978, **40**, 45–62.
15. Hein, J. R. and Morgan, C. L., *Deep-Sea Res.*, 1999, **46**, 855–875.
16. Burns, R. G. and Burns, V. M., in *Marine Manganese Deposits* (ed. Glassby, G.), Elsevier, The Netherlands, 1977, pp. 185–244.
17. Lalou, C. (ed.), Proc. Intl. Collq. No. 289 on a 'La Genese des Nodules de Manganese', CNRS Paris, France, 1979.
18. Cronan, D. S., in *Marine Manganese Deposits* (ed. Glassby, G. P.), Elsevier, NY, 1976, pp. 11–14.
19. Barnes, S. S., *Science*, 1967, **157**, 63–65.
20. Calvert, S. E. and Price, N. B., *Mar. Chem.*, 1977, **5**, 43–74.
21. Goldberg, E. D., *J. Geol.*, 1954, **62**, 249–265.
22. Goldberg, E. D. and Arrhenius, G. O. S., *Geochim. Cosmochim. Acta*, 1958, **13**, 153–212.
23. Bonatti, E. and Nayudu, Y. R., *Am. J. Sci.*, 1965, **263**, 17–39.
24. Lal, D. and Peters, B., *Handb. Phys.*, 1967, **46**, 551–612.
25. McHargue, L. R. and Damon, P. E., *Rev. Geophys.*, 1991, **29**, 141–158.
26. Amin, B. S., Lal, D. and Somayajulu, B. L. K., *Geochim. Cosmochim. Acta*, 1975, **39**, 1187–1192.
27. Goldberg, E. D. and Koide, M., *Geochim. Cosmochim. Acta*, 1962, **26**, 417–450.
28. Merrill, J. R., Lyden, E. F. X., Honda, M. and Arnold, J. R., *Geochim. Cosmochim. Acta*, 1969, **18**, 108–129.

29. Somayajulu, B. L. K., *Science*, 1967, **156**, 1219–1220.
30. Guichard, F., Reyss, J-L. and Yokoyama, Y., *Nature*, 1978, **272**, 155–156.
31. Bhat, S. G., Krishnaswami, S., Lal, D., Rama and Somayajulu, B. L. K., in Proceedings of the Conference on Hydrogeochemistry and Biogeochemistry, Tokyo, Japan, 1970, The Clarke & Co., Washington, DC, 1973, vol. 2, pp. 443–462.
32. Ku, T. L., Omura, A. and Chen, P. S., in *Marine Geology and Oceanography of the Pacific Manganese Nodule Province* (eds Bischoff, J. L. and Piper, D. Z.), Plenum Press, NY, 1979, pp. 791–814.
33. Inoue, T., Huang, Z-Y, Imamura, M., Tanaka, S. and Usui, A., *Geochem. J.*, 1983, **17**, 307–312.
34. Raisbeck, G. M., Yiou, F., Fruneau, M. and Loiseux, J. M., *Science*, 1978, **202**, 214–217.
35. Sharma, P. and Somayajulu, B. L. K., *Indian J. Mar. Sci.*, 1983, **12**, 174–176.
36. Belshaw, N. S., O'Nions, R. K. and Von Blanckenburg, F., *Int. J. Mass Spectrom. Ion Phys.*, 1995, **142**, 55–67.
36a. Tuniz, C., Bird, J. R., Fink, D. and Herzog, G. F., *Accelerator Mass Spectrometry*, CRC Press, Boca Raton, USA, 1998, p. 371.
37. Sharma, P., Ph D thesis, PRL, Gujarat University, 1982, p. 196.
38. Mangini, A., Segl, M., Kudrass, H., Wiedickel, M., Bonani, G., Hofman, H. J., Morenzoni, E., Nessi, M., Suter, M. and Wolfli, W., *Geochim. Cosmochim. Acta*, 1986, **50**, 149–156.
39. Ku, T. L., Kusakabe, M., Nelson, D. E., Southon, J. R., Korteling, R. G., Vogel, J. and Nowikow, I., *Nature*, 1982, **299**, 240–242.
40. Ingram, B. L., Hein, J. R. and Farmer, G. L., *Geochim. Cosmochim. Acta*, 1990, **54**, 1709–1721.
41. McMurty, G. M., VonderHaar, D. L., Eisenhauer, A., Mahoney, J. J. and Yeh, H.-W., *Earth Planet. Sci. Lett.*, 1994, **125**, 105–118.
42. Sharma, P. and Somayajulu, B. L. K., *Earth Planet. Sci. Lett.*, 1982, **59**, 235–244.
43. Krishnaswami, S., Mangini, A., Thomas, J. H., Sharma, P., Cochran, J. K., Turekian, K. K. and Parker, P. D., *Earth Planet. Sci. Lett.*, 1982, **59**, 221–234.
44. Sharma, P., Somayajulu, B. L. K., Lal, D., Wolfli, W., Bonani, G., Stoller, Ch., Suter, M. and Beer, J., *Proc. Indian Acad. Sci.*, 1983, **92**, 1–4.
45. Ling, H. F., Burton, K. W., O'Nions, R. K., Kaluber, B. S., Von Blanckenburg, F., Gibb, A. J. and Hein, J. R., *Earth Planet. Sci. Lett.*, 1997, **146**, 1–12.
46. Von Blanckenburg, F. and O'Nions, R. K., *Earth Planet. Sci. Lett.*, 1999, **167**, 175–182.
47. Ku, T. L. and Broecker, W. S., *Deep-Sea Res.*, 1969, **16**, 625–637.
48. Moore, W. S., Ku, T. L., Macdougall, J. D, Burns, V. M., Burns, R., Dymond, J., Lyle, M. and Piper, D. Z., *Earth Planet. Sci. Lett.*, 1981, **52**, 151–171.
49. Moore, W. S. and Vogt, P. R., *Earth Planet. Sci. Lett.*, 1976, **9**, 349–356.
50. Kennett, J. P. and Watkins, N. D., *Science*, 1975, **188**, 1011–1013.
51. Paul, A. Z., Throndike, E. M., Sullivan, L. G., Heezen, B. C. and Gerad, R. D., *Nature*, 1978, **272**, 812–814.
52. Banse, K., in *Biogeochemistry of the Arabian Sea* (ed. Lal, D.), Indian Academy of Sciences, Bangalore, India, 1994, pp. 27–63.
53. Murali, A. V., Blanchard, D. P., Somayajulu, B. L. K. and Parekh, P. P., *EOS*, Abstract, 1987, **66**, 1320.
54. Murali, A. V., Parekh, P. P. and Cumming, J. B., *Geochim. Cosmochim. Acta*, 1990, **54**, 889–894.
55. Vol Blankernburg, F., O'Nions, R. K., Belshaw, N. S., Gibb, A. and Hein, J. R., *Earth Planet. Sci. Lett.*, 1996, **141**, 213–226.
56. Krishnaswami, S., Trivedi, J. R., Sarin, M. M., Ramesh, R. and Sharma, K. K., *Earth Planet. Sci. Lett.*, 1992, **109**, 243–253.
57. Higdon, J. C. and Lingenfelter, R. E., *Nature*, 1973, **246**, 403–405.
58. Forman, M. A. and Schaeffer, P. A., *Rev. Geophys. Space Phys.*, 1979, **17**, 552–560.
59. Somayajulu, B. L. K., *Geochim. Cosmoschim. Acta*, 1977, **41**, 909–913.
60. Sharma, P., Bhattacharya, S. K. and Somayajulu, B. L. K., Proceedings of the 18th International Cosmic Ray Conference, Bangalore, India, 1983, vol. 2, pp. 337–340.
61. Turekian, K. K. and Luck, J-M., *Proc. Natl. Acad. Sci. USA*, 1984, **81**, 8032–8034.
62. Chan, L. S., Chu, C. L. and Ku, T. L., *Geophys. J. R. Astron. Soc.*, 1985, **80**, 715–723.
63. Kok, Y. S., *Earth Planet. Sci. Lett.*, 1999, **166**, 105–119.
63a. Robinson, C., Raisbeck, G. M., Yiou, F., Lehman, B. and Laj, C., *Earth Planet. Sci. Lett.*, 1995, **136**, 551–557.
64. Banerjee, R., Roy, S., Dasgupta, S., Mukhopadhyay, S. and Miura, H., *Mar. Geol.*, 1999, **157**, 145–158.
65. Roonwal, G. S., *The Indian Ocean: The Exploitable Mineral and Petroleum Resources*, Springer-Verlag, Berlin, 1986.
66. Sudhakar, M., Kodagali, V. N. and Jai Sankar, S., Proceedings of the 28th Annual Off-Shore Technology Conference, Houston TX, 1996, pp. 475–483.
67. Luck, J. M. and Turekian, K. K., *Science*, 1983, **222**, 613–615.
68. Sorem, R. K. and Foster, A. R., in *Ferromanganese Deposits on the Ocean Floor* (ed. Horn, D. R.), LDGO, NY, NSF/IDOE, Washington D.C., 1972, pp. 167–181.
69. Krishnaswami, S., Somayajulu, B. L. K. and Moore, W. S., in Proceedings of the Conference on Ferromanganese Deposits on the Ocean Floor (ed. Horn, D. R.), LDGO, NSF/IDOE, Washington, DC, 1972, pp. 117–122.
70. Harriss, R. C., Crocket, J. H. and Stainton, M., *Geochim. Cosmochim. Acta*, 1968, **32** 1049–1056.
71. Elderfield, H., Hawkesworth, C. J., Greaves, M. J. and Calvert, S. E., *Geochim. Cosmochim. Acta*, 1981, **45**, 513–528.
72. Manahein, F. T., *Science*, 1986, **232**, 600–608.
73. Palmer, M. R., Falkner, K. K. and Turekian, K. K., *Geochim. Cosmochim. Acta*, 1988, **52**, 1197–1202.
74. Cumming, J. B., Murali, A. V., Parekh, P. P. and Somayajulu, B. L. K., 2000 (manuscript under preparation).
75. Lawrence Edwards, R., Chen, J. H. and Wasserburg, G. J., *Earth Planet. Sci. Lett.*, 1986, **81**, 175–192.
76. Anderson, M. E. and Macdougall, J. D., *Geophys. Res. Lett.*, 1977, **4**, 351–353.
77. Faure, G., *Principles of Isotope Geology*, John Wiley, NY, 1986.
78. Middleton, R. and Klein, J., *Philos. Trans. R. Soc. London*, 1987, **323**, 121–143.
79. Lyle, M., *Geochim. Cosmochim. Acta*, 1982, **46**, 2301–2306.
80. Halback, P., Segl, M., Puteaunus, D. and Mangini, A., *Nature*, 1983, **304**, 716–719.
81. Hein, J. R., Bohrson, W. A., Schutz, M. S., Noble, M. and Clague, D. A., *Palaeooceanography*, 1992, **7**, 63–77.
82. Crecelius, E. A., Carpenter, R. and Merrill, R. T., *Earth Planet. Sci. Lett.*, 1973, **17**, 391–396.
83. Barnes, S. S. and Dymond, J. R., *Nature*, 1967, **213**, 1218–1219.
84. Kvenvolden, K. A. and Blunt, D. J., in *Marine Geology and Oceanography of the Pacific Manganese Nodule Province* (eds Bischoff, J. L. and Piper, D. Z.), Plenum Press, NY, 1979, pp. 763–773.
85. Bada, J. L., *Earth Planet. Sci. Lett.*, 1972, **15**, 223–231.

ACKNOWLEDGEMENTS. I thank Dr S. R. Shetye, NIO, Mr Ravi Bhushan and Ms. Pauline Joseph, PRL. I am indebted to Dr M. Sudhakar of the National Centre for Antarctic and Ocean Research, Goa for providing Figure 1 and some literature. The encouragement received from PRL and CSIR through the posts of Honorary Professor and Emeritus Scientist is acknowledged.